

Recent Improvements to STIS Pipeline Calibration

Rosa I. Diaz-Miller, Jessica Kim Quijano, Jeff A. Valenti, Charles R. Proffitt, Kailash C. Sahu, Ralph C. Bohlin, Thomas M. Brown

Space Telescope Science Institute, 3700 San Martin Drive, Baltimore, MD 21218

Don Lindler

Computer Science Corporation, Inc.

Abstract. In the last few months a number of improvements to the STIS pipeline calibration have been developed and implemented, which include the following.

We have released new low order flat files for use with the G140L observations. These flats should reduce uncertainties of the extracted flux with position from 12% to 2%.

To better reflect the change with time in the overall shape of the NUV MAMA dark current, new dark reference files were created for different epochs. To further improve the dark subtraction, these darks are also scaled using an improved algorithm, which takes into account long term changes in the behavior of the NUV MAMA dark current.

Additional improvements which have been implemented are described in the posters by Stys et al., Valenti et al., Davies et al. and Lindler et al. Future improvements include background smoothing for low signal spectroscopic data, and updating the Pixel-to-Pixel flat library and the current CCD bad pixel table.

1. New Low Order Flat Image File for G140L

As part of STIS calibration program 7937, observations of the spectrophotometric standard star GD 71 were taken at 20 different positions along the length of the $52 \times 2''$ slit, and showed significant variation in sensitivity with position. These discrepancies in the extracted flux relative to a point source at the standard position are as large as 12%. To correct for this, new LFLATs (lfl files) were prepared using the 7937 observations. Use of these new lfl files should reduce these discrepancies to 2% or less, except when the spectrum falls across the shadow of the FUV MAMA's repeller wire.

Prior to March 15, 1999, G140L spectra were shifted $3''$ above the repeller wire, while after this date the default position was changed to $3''$ below the repeller wire. Different sensitivity calibrations are applied before and after this date to correct for the differences between the two positions. One new lfl file was prepared for each of these epochs and normalized to unity near the appropriate standard extraction position.

Figure 1 (left) shows the ratio of the extracted count rates from the 7937 observations of GD 71 to a reference spectrum, both with and without the application of this new LFLAT. The same star was also observed at a more limited number of positions as part of program 7097. The 7097 data were not used to constrain the LFLAT, and while the scatter is larger than for the 7937 data, the improvement is still significant (Figure 1, right).

2. New MAMA Dark Reference Files

The NUV MAMA dark current is dominated by phosphorescence from impurities in the detector window. Cosmic rays excite electrons in these impurities into metastable states, which can be

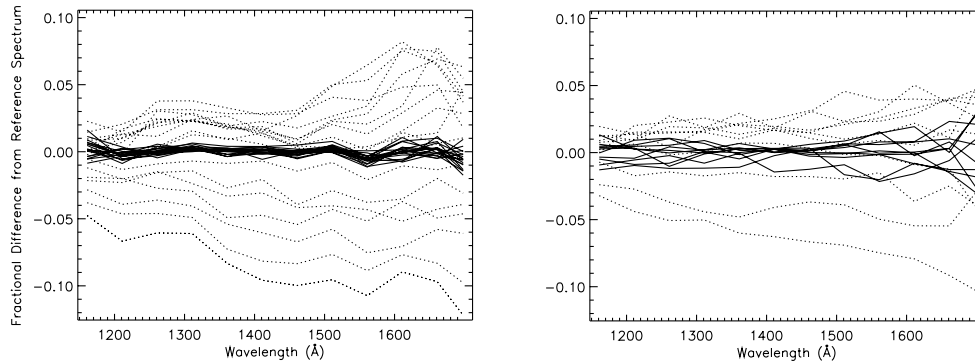


Figure 1. Count rate comparison after using new G140L LFLAT (solid lines) and without it (dashed lines). GD 71 observations: program 7930 (left) and program 7097 (right).

collisionally excited to unstable states that then decay by emitting UV photons. This process can be modeled by the equation:

$$\text{rate} = \text{constant} * \text{number of excited states} * \exp(-\delta E/kT) \quad (1)$$

In addition to the variations in the overall level of the dark current which have been discussed elsewhere (Ferguson & Baum 1999), there has been a subtle change over time in the relative intensities of this dark current at different places on the NUV MAMA detector. To better reflect this change in the overall shape of the NUV MAMA dark, four new dark files were created; each intended for use with NUV MAMA data during a given time period.

On the other hand, the original NUV dark scaling formula used in the pipeline assumed that the number of excited states could be well approximated by a constant value, and adopted fixed coefficients for this formula. However, long term changes in the mean operating temperature of the detector can significantly change the equilibrium population of excited states. In addition, it is observed that the dark current at the lowest detector temperatures does not drop as low as the original formula would predict. This may indicate that there are other sources of dark current with different time scales and thermal characteristics.

To better model the dark current, formula (1) was changed to allow the overall normalization to vary slowly over time to represent the long term evolution of the number of excited metastable states, and to impose a lower limit to the temperature used in this formula. This minimum temperature was also allowed to vary with time. These coefficients, as well as other coefficients in the equation which are currently left fixed, are read into Calstis from the TDC table, a new STIS reference file type, which contains the adopted coefficients as a function of time.

Dark monitor observations were used to calibrate these coefficients, and it was found that using the modified formula substantially reduces the discrepancy between observed and predicted rates. The NUV dark current predicted by the revised formula should be within 5% of the correct value about 85% percent of the time, and within 10% about 95% of the time (see Figure 2). To maintain this accuracy as the mean thermal condition of the detector changes, periodic updates to the TDC table will be necessary.

3. Smoothing the Background in STIS Spectroscopic Data

For low signal data, it is advantageous to smooth the background since such a smoothing can decrease the background noise level, and hence improve the quality of the results. In addition to the

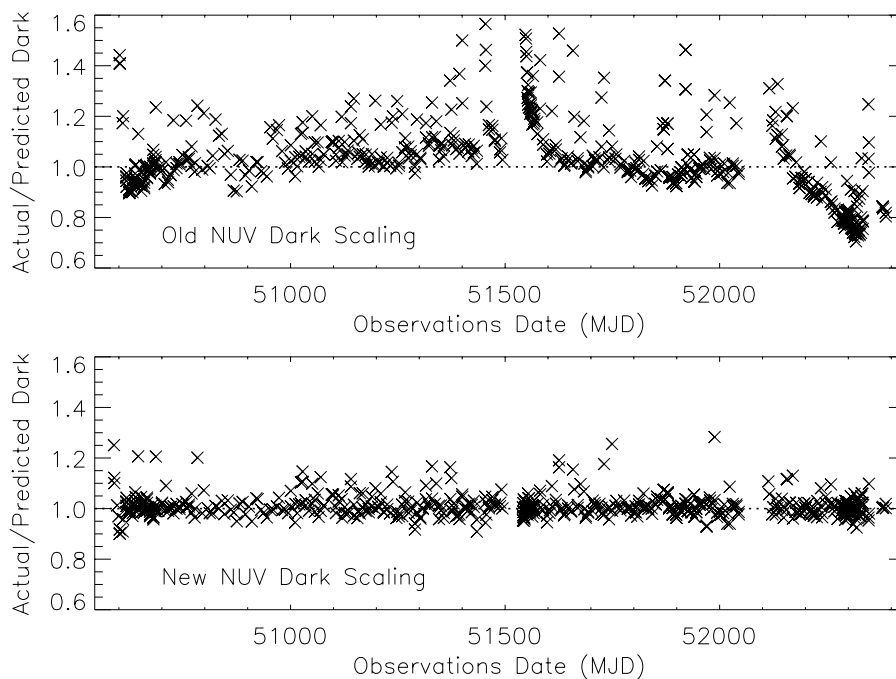


Figure 2. Comparison observed and predicted NUV-MAMA dark rate using the old (top) and the new (bottom) NUV dark scaling formula.

smoothing that is currently being done in the pipeline in the cross-dispersion direction, we are implementing additional smoothing in the dispersion direction by fitting a polynomial of order 3 to the background. In this procedure, we exclude the region occupied by the geo-coronal lines in the fit (in the UV-region), and for these regions use the simple row-averaged background instead.

Figure 3 shows the results before and after the background smoothing algorithm is applied: the results are slightly better after the smoothing. The figure at the bottom shows the ratio of the flux before and after smoothing, which is close to 1 as expected.

4. Updating the Pixel-to-Pixel Flat Library

We have created new p-flats (pixel-to-pixel, high-frequency flats) for the STIS MAMAs. These p-flats combine the data from four years of lamp exposures to achieve a signal-to-noise ratio of 200 per low-resolution pixel (compared with a signal-to-noise ratio of 100 in the extant p-flats). Details on the creation of these P-flats can be found in Brown & Davies (2002).

5. MAMA Bad Pixel Table

The MAMA bad pixel mask (in the Data Quality extension) will be updated to reflect the true occulted regions on each detector (notably the horizontal repeller shadow across the middle of the far-UV detector and the corners of the near-UV detector). Currently, the DQ extension reflects the bad pixels in the G140M and G230M modes, which is not appropriate for the other spectroscopic and imaging modes. Furthermore, the bad pixel mask changes somewhat with time due to changes in the Mode Select Mechanism position over the course of the mission. Thus, the new Data Quality flags will be mode- and time-dependent.

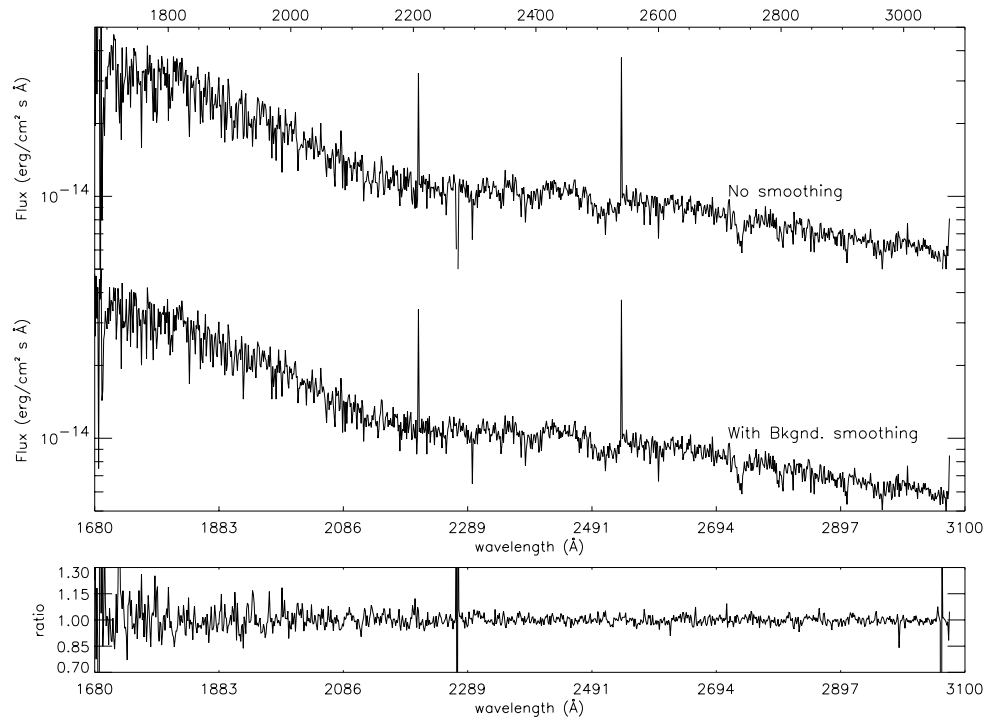


Figure 3. Top: Spectrum before and after the background smoothing. Bottom: Ratio of the flux before and after smoothing.

References

- Brown, T. M. & Davies, J. E. 2002, *Technical Instrument Report STIS 2002-03* (Baltimore: STScI)
Ferguson, H. & Baum, S. 1999, *Instrument Science Report STIS 99-02* (Baltimore: STScI)